European Radiology
https://doi.org/10.1007/s00330-020-07055-6

MAGNETIC RESONANCE

Plaque characteristics of middle cerebral artery assessed using strategically acquired gradient echo (STAGE) and vessel wall MR contribute to misery downstream perfusion in patients with intracranial atherosclerosis

Tong Zhang[1,2] · Ruowei Tang[1,2] · Song Liu[1,2] · Chao Chai[1,2] · Yongsheng Chen[3,4] · E. Mark Haacke[3,4] · Shuang Xia[2]

Received: 11 February 2020 / Revised: 21 April 2020 / Accepted: 30 June 2020

Abstract

Objectives To assess plaque vulnerability of the middle cerebral artery (MCA) using strategically acquired gradient echo (STAGE) versus high-resolution vessel wall MRI (hr-vwMRI), and explore the relationship between plaque characteristics and misery downstream perfusion.

Methods Ninety-one patients with single MCA atherosclerotic plaques underwent STAGE and hr-vwMRI were categorized into a group with misery perfusion and a group without based on the Alberta Stroke Program Early CT score (MTT-ASPECTS) with a threshold of 6. Plaque characteristics including inner lumen area (IWA), susceptibility, presence of hyperintensity within plaque (HIP), surface irregularity, stenosis degree, remodeling index, lipid ratio, and enhancement grade were compared between the two groups. The vulnerability of each plaque was retrospectively assessed on both STAGE and hr-vwMRI according to the combination of plaque features. Logistic regression analysis and ROC curve were performed to evaluate the effect of plaque characteristics on the presence of misery perfusion.

Results Taking hr-vwMRI as the reference, STAGE showed good efficiency in detecting vulnerable plaques. Patients with misery perfusion had less IWA, higher stenosis degree, more irregular surface and HIP, higher enhancement grade, and susceptibility ($p < 0.01$ for all). Higher susceptibility and stenosis degree were independent predictors for the occurrence of misery perfusion ($p = 0.025$, $p = 0.048$). The AUC was 0.900 for the combination of the two variables.

Conclusion STAGE shows good efficiency to assess MCA plaque vulnerability versus hr-vwMRI. Plaque susceptibility evaluated using STAGE provides incremental value to predict misery perfusion combined with hr-vwMRI plaque features.

Key Points

- *STAGE has good efficiency in evaluating MCA plaque vulnerability* versus *hr-vwMRI.*
- *Higher plaque susceptibility assessed using STAGE and higher grade luminal stenosis based on hr-vwMRI attribute to misery downstream perfusion.*
- *STAGE provides incremental value on the understanding of plaque vulnerability in addition to conventional hr-vwMRI.*

Keywords Atherosclerotic plaques · Middle cerebral artery · Perfusion · Brain mapping

Electronic supplementary material The online version of this article (https://doi.org/10.1007/s00330-020-07055-6) contains supplementary material, which is available to authorized users.

✉ Shuang Xia
xiashuang77@163.com

[1] Radiology Department, First Central Clinical College, Tianjin Medical University, Tianjin, China

[2] Radiology Department, Tianjin First Central Hospital, Number 24 of Fukang Road, Nankai District, Tianjin, China

[3] The MRI Institute for Biomedical Research, Detroit, MI, USA

[4] Department of Radiology, Wayne State University, Detroit, MI, USA

Published online: 01 August 2020

Abbreviations

DSC-PWI	Dynamic susceptibility contrast perfusion-weighted imaging
DWI	Diffusion-weighted imaging
HP-phase	High-pass phase
hr-vwMRI	High-resolution vessel wall MRI
IPH	Intraplaque hemorrhage
IR-SPACE	Inversion-Recovery prepared Sampling Perfection with Application-optimized Contrast using different flip angle Evolutions
MCA	Middle cerebral artery
MTT-ASPECTS	Mean transit time maps according to the Alberta Stroke Program Early CT score
QSM	Quantitative susceptibility mapping
SPIN	Signal processing in nuclear magnetic resonance
STAGE	Strategically acquired gradient echo
SWI	Susceptibility-weighted imaging

Introduction

Intracranial atherosclerotic disease (ICAD) caused by vulnerable plaques in the middle cerebral artery (MCA) are common in Asians [1]. Neovascularization, necrotic lipid core, and inflammatory infiltration have been proven to promote the development of plaque instability and disruption [2–4]. Therefore, assessing plaque vulnerability before the occurrence of cerebrovascular events is vital for therapy and prognosis. Different from traditional intracranial lumenography approaches such as digital subtraction angiography (DSA), computed tomography angiography (CTA), ultrasound, and time-of-flight magnetic resonance angiography (TOF-MRA), high-resolution vessel wall MRI (hr-vwMRI) directly depicts vessel wall, providing advantages on evaluating plaque morphologic characteristics and vulnerability [5–7].

Hypoperfusion is one of the probable mechanisms of ischemic stroke [8, 9]. Mean transit time (MTT) maps originated from dynamic susceptibility contrast perfusion-weighted imaging (DSC-PWI) is sensitive to reflect hypoperfusion of the cerebral tissues [10]. However, the relationship between plaque vulnerability and hypoperfusion remains controversial and complicated. Disruption of vulnerable plaques and severe luminal stenosis caused by stable plaques may both attribute to misery perfusion. Studies have demonstrated that less eccentric and strongly enhanced plaques are associated with the occurrence of misery perfusion [11, 12], while the impact of other vulnerable plaque features and components such as intraplaque hemorrhage (IPH) and irregular surface on the downstream perfusion is still unclear. Therefore, a new imaging protocol is needed to facilitate the investigation performed using hr-vwMRI.

Susceptibility-weighted imaging (SWI) is an emerging MR method to visualize vessel walls, and the use of phase or reconstructive quantitative susceptibility mapping (QSM) has the potential for differentiating calcium from blood because of their differences in susceptibility [13–15]. The QSM data makes the quantitative measurement of susceptibility in the brain possible [16, 17]. Previous studies have shown that QSM can be used for measuring iron content and oxygen saturation from major veins but its applications in intracranial arteries are limited [14, 18, 19]. A newly developed rapid multi-contrast protocol referred as strategically acquired gradient echo (STAGE) imaging can provide structural (STAGE-A) and angiographic (STAGE-B) information in roughly 5 min each [20, 21]. In STAGE-B, one can obtain arterial angiograms as well as SWI data to help distinguish blood from calcium in the brain [22]. We hypothesized that (1) QSM images processed from STAGE-B were sensitive to detect vulnerable and stable plaques which generated focal susceptibility change, and (2) quantitative plaque susceptibility measured on QSM as well as plaque features evaluated on hr-vwMRI was associated with the presence of downstream misery perfusion.

The purposes of this study were as follows: (1) to investigate the efficiency in evaluating vulnerability of MCA plaques for STAGE-B compared with hr-vwMRI in patients with ICAD; (2) to explore the relationship between plaque characteristics assessed using STAGE and hr-vwMRI and the misery downstream perfusion.

Materials and methods

Patient population

This study was approved by our institutional review board ethic committee. Written informed consent was obtained from each patient before the MR examination. We retrospectively analyzed 732 patients admitted to our hospital between September 2016 and December 2019, all of whom had undergone hr-vwMRI examinations. Finally, 91 patients were included in this study according to the following inclusion criteria: (1) patients who had STAGE-B data collected at the same time as the hr-vwMRI and DSC-PWI data; (2) patients with symptoms of ICAD in the territory of MCA; (3) patients with single and unilateral atherosclerotic plaque located in the MCA verified by hr-vwMRI; and (4) no evidence of cardioembolism. Exclusion criteria included the following: (1) nonatherosclerotic vasculopathies, including vasculitis, moyamoya disease, aneurysm, dissection, and intramural hematoma diagnosed by TOF-MRA, hr-vwMRI, and clinical evaluation; (2) multiple plaques or no plaque existing in the MCA diagnosed by hr-vwMRI; (3) ipsilateral internal carotid arterial (ICA) stenosis more than 30% based on MRA or

DSA; (4) insufficient image quality caused by motion artifact; or (5) poor data. A detailed flowchart of patient inclusion and exclusion is given in Fig. 1. Patients' clinical information, including cerebrovascular risk factors, time interval from onset to MR scan, and National Institutes of Health Stroke Scale (NIHSS), were collected (see Table 1).

MRI protocol

All patients were scanned on a 3.0-T Siemens Prisma scanner (Siemens Medical Systems) using a 64-channel head-neck coil. A 3D Inversion-Recovery prepared Sampling Perfection with Application-optimized Contrast using different flip angle Evolutions (IR-SPACE) was performed to acquire vessel wall images with the resolution of 0.55 × 0.55 × 0.55 mm. STAGE-B was performed to create QSM data to evaluate plaque vulnerability. The resolution is 0.67 × 0.67 × 2 mm. DSC-PWI with a dose of 0.1 mmol/kg gadoteric acid were performed to generate MTT images and evaluate the degree of misery perfusion. Post-contrast IR-SPACE was acquired right after DSC-PWI. DWI was performed to determine the presence of acute ischemic stroke. Detailed parameters of the sequences are described in Supplementary Table 1.

Image processing

STAGE data was processed using signal processing in nuclear magnetic resonance (SPIN) software. A 96 × 96 filter was utilized to generate high-pass phase (HP-phase) images. The reconstruction of QSM images was performed using STAGE processing software (STAGE version 2.1.4) with the following steps: skull removal using brain extraction tool (BET), phase unwrapping, phase quality map, background field removal using sophisticated harmonic artifact reduction for phase data (SHARP) algorithm, and an inverse filter with a k-space threshold of 0.1 [16, 23, 24].

MTT maps originated from raw DSC-PWI images were reconstructed using the singular value decomposition deconvolution method, and the arterial input function for MTT estimation was selected from the contralateral MCA [25].

Image analysis

Two radiologists, both with more than 2 years' experience and both blinded to clinical information, analyzed the vessel wall and STAGE images independently. Misery perfusion was visually evaluated by another two experienced observers blinded to other images using a 10-point MTT-Alberta Stroke Program Early CT

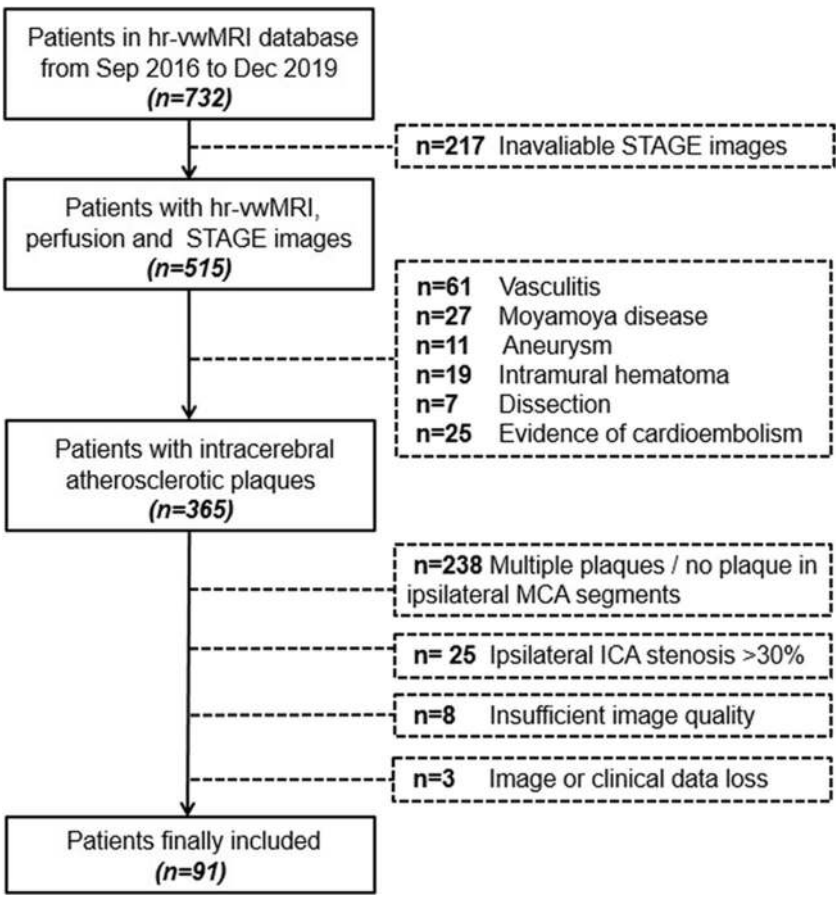

Fig. 1 Flowchart displaying the selection of patients

Table 1 Patient demographics

	Total ($n = 91$)	Group with misery perfusion ($n = 29$)	Group without misery perfusion ($n = 62$)	p value
Age, mean (range) *y*	60.12 ± 11.92	58.55 ± 13.54	60.85 ± 11.12	0.393
Male sex, *n* (%)	64 (70.33)	19 (65.52)	45 (72.58)	0.492
Hypertension, *n* (%)	59 (64.84)	18 (62.07)	41 (66.13)	0.705
Hyperlipidemia, *n* (%)	11 (12.09)	3 (10.34)	8 (12.90)	0.727
Diabetes mellitus, *n* (%)	29 (31.87)	12 (41.38)	17 (27.42)	0.183
Active smoker, *n* (%)	35 (38.46)	10 (34.48)	25 (40.32)	0.594
Alcohol user, *n* (%)	35 (38.46)	13 (44.83)	22 (35.48)	0.393
DWI-positive stroke, *n* (%)	36 (39.56)	20 (68.97)	16 (25.81)	< 0.001
Time interval between onset and MR scan, days	13.05 ± 8.98	10.45 ± 5.43	14.27 ± 10.04	0.058
NIHSS	1.00 (0.00–3.00)	3.00 (0.00–6.00)	0.50 (0.00–2.00)	0.001

All data are *n* or mean ± SD or median (interquartile ranges)

NIHSS, National Institutes of Health Stroke Scale

score (MTT-ASPECTS) (11) (see supplementary methods and Supplementary Fig. 2). Based on the MTT-ASPECTS, all patients were categorized into two groups: one with misery perfusion (MTT-ASPECTS ≤ 6) and one without misery perfusion (MTT-ASPECTS > 6) [11, 26, 27].

All quantitative data were measured three times individually to obtain the mean value and re-measured two weeks later by reader 1 for the intra-observer and inter-observer reproducibility assessments.

Plaque characteristics based on hr-vwMRI

The 3D vessel wall images were reconstructed and analyzed on a Picture Archiving and Communication Systems (PACS) workstation. Images were reconstructed using the 3D multiplanar reconstruction (MPR) tool of the PACS system, and plaques were evaluated on slices perpendicular to the long and short axes of MCA vessels (see Supplementary Fig. 1). Plaques were defined as the vessel wall lesions whose thickness was 1.5 times greater than that of the contralateral normal walls. The reference lumen was defined as the nearest plaque-free MCA segments proximal (which is the first choice) or distal (second choice) to the maximal lumen narrowing (MLN) cross-section [28]. Measurements of plaque characteristics including outer wall area (OWA), inner wall area (IWA), lesion area (LA), and plaque length were demonstrated in supplementary methods and Supplementary Fig. 1. Other plaque characteristics were evaluated as follows:

1) Remodeling index = OWA_{lesion} / $OWA_{reference}$ [12];
2) Stenosis degree = (1-IWA_{lesion} / $IWA_{reference}$) × 100%;
3) Hyperintensity within plaque (HIP) was defined as the maximal signal intensity (SI) within the plaque on the pre-contrast image 150% higher than that of the reference wall [29];
4) Surface irregularity: the inner surface of plaque adjacent to lumen was smooth (regular/0), or not smooth (irregular/1);
5) Lipid area: area of SI_{lesion} / $SI_{reference}$ < 150% on the post-contrast image; demonstrations of HIP, surface irregularity, and lipid area were shown in Fig. 2.
6) Lipid ratio (LR) = lipid area / LA × 100%;
7) Enhancement grade: was assessed on the post-contrast HR-VWI images as follows: grade 0, $SI_{lesion} = SI_{reference}$; grade 1, $SI_{reference} < SI_{lesion} < SI_{pituitary\ infumdibulum}$; grade 2, $SI_{lesion} \geq SI_{infundibulum}$ [30].

Based on previous research, vulnerability of each plaque was evaluated following a combination of 2 major criteria: (a) presence of HIP; (b) irregular surface (each has a 3-point weighing); and 4 minor criteria: (c) grade 2 enhancement; (d) stenosis degree > 50%; (e) remodeling index < 0.95; (f) LR > 50% (each has a 1-point weighing) [12, 29, 31–34]. Total weighing for vulnerability (TWV) was calculated for each plaque. Plaque was defined as vulnerable if TWV ≥ 5, or stable if TWV < 5.

Plaque evaluation based on STAGE

STAGE images were analyzed using SPIN. Axial images of different STAGE sequences were zoomed in and co-registered with identical field of view (FOV). Focal susceptibility change generated by different plaque components was defined as local hypointensity on magnitude, hypo- or hyperintensity on phase, HP-phase, and QSM images with plaque situated along MCA walls as confirmed by hr-vwMRI (see Fig. 2). Local abnormal signal caused by susceptibility change was drawn manually on QSM images as areas with clear contours distinct from adjacent wall. And the mean value of susceptibility for

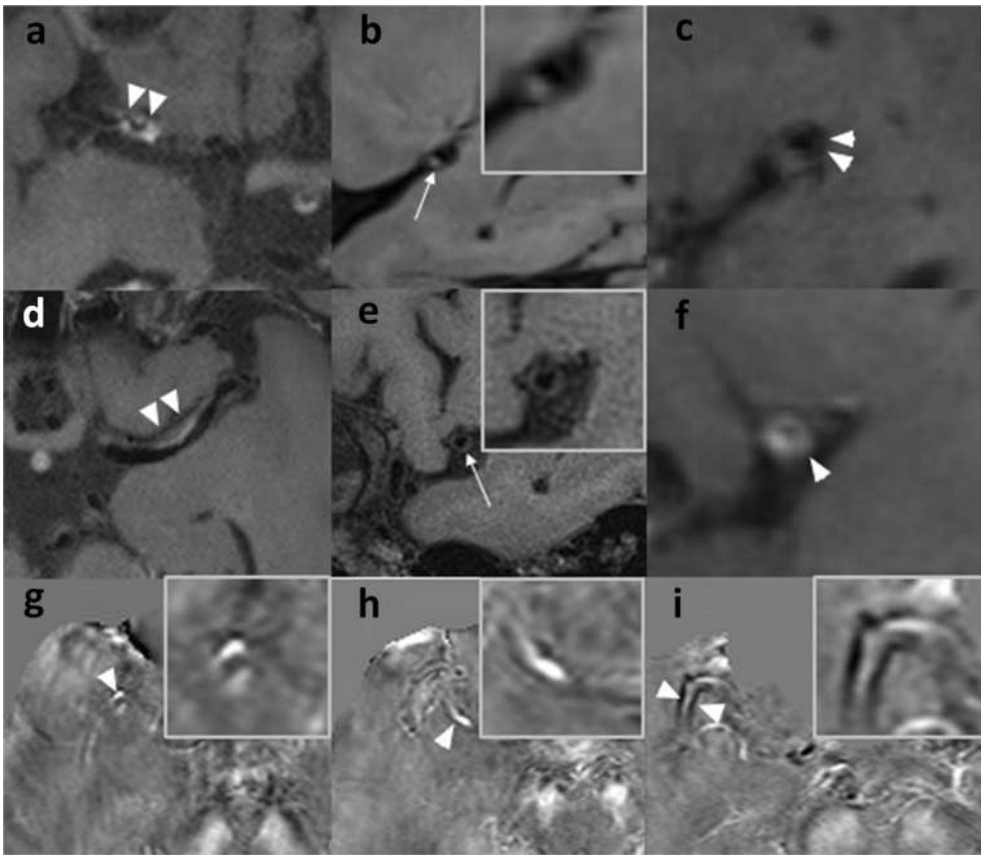

Fig. 2 Demonstrations of surface irregularity, presence of HIP, lipid area, and plaque signals on QSM images. Arrowheads indicates irregular plaque surface (**a**) and regular (**d**); large hypointensity suggesting lipid within the plaque on the sagittal cross-section (**c**) and no hypointensity (**f**); two examples of bright plaque signal (**g**, **h**) and dark plaque signal (**i**) in the right M1 segment on the QSM images. Arrows show hyperintensity within plaque on the pre-contrast vw-MRI (**b**), and no hyperintensity (**e**)

each lesion was automatically calculated by SPIN. Based on QSM results, each plaque was defined as vulnerable (with positive susceptibility) or stable (with negative susceptibility).

Statistical analysis

All statistical analyses were performed using SPSS software (v. 22.0). Whether all continuous variables were normally distributed was tested using the Kolmogorov-Smirnov test. Continuous variables were presented as mean ± standard deviations (SD) or median and interquartile range (IQR) based on data distribution pattern. Comparisons of continuous variables and categorical variables among the patient groups were conducted via Student's *t* test, Mann-Whitney *U* test, and chi-square test as appropriate. The intra-observer and inter-observer reproducibility for plaque characteristics and MTT-ASPECTS was assessed using intraclass correlation coefficient (ICC), weighted Kappa, and Cohen κ as appropriate. The relationships between plaque characteristics and MTT-ASPECTS, susceptibility, and TWV were analyzed using Spearman correlation analysis. Multivariate logistic regression was applied to identify plaque characteristics affecting misery perfusion at $p < 0.1$ level in univariate analyses. Receiver operating characteristic (ROC) curve and area under curve (AUC) were performed to test the diagnosis efficiency for the significant variables to predict misery perfusion. The ROC curves were created by MedCalc Statistical Software version 18.2.1 (MedCalc Software bvba). $p < 0.05$ was considered statistically significant.

Results

Patients demographic data

Of 732 patients initially imaged, 91 who met the inclusion/exclusion criteria patients were included (Fig. 1). Twenty-nine patients were in the group with misery perfusion and 62 in the group without. Thirty-six patients had acute infarction and 55 had transient ischemic attack (TIA). The patient group with misery perfusion had higher frequency of DWI-positive acute stroke and higher NIHSS ($p < 0.001$, $p = 0.001$). Other patient characteristics showed no differences between the two groups (Table 1). Results of data distribution pattern were listed in Supplementary Table 2.

Inter-observer and intra-observer reproducibility

Inter-observer and intra-observer reproducibility for plaque characteristics and MTT-ASPECTS were highly consistent (see Supplementary Table 3).

Table 2 Comparisons of plaque characteristics between the groups with and without misery perfusion

Plaque characteristics	Patients with misery perfusion ($n = 29$)	Patients without misery perfusion ($n = 62$)	p value
OWA (mm^2)	4.48 (2.90–6.32)	4.98 (3.97–7.35)	0.240
IWA (mm^2)	0.54 (0.26–1.02)	0.99 (0.70–1.82)	0.002
LA (mm^2)	3.92 (2.23–5.34)	4.07 (2.90–5.07)	0.851
Stenosis degree (%)	82.00 (67.00–85.95)	66.00 (46.15–75.90)	< 0.001
Remodeling index	0.92 (0.74–1.12)	0.90 (0.78–1.20)	0.506
Lipid area (mm^2)	0.20 (0.00–0.61)	0.47 (0.00–1.31)	0.164
LR (%)	5.60 (0.00–17.61)	15.57 (0.00–29.50)	0.137
Plaque length (mm)	5.65 (3.84–6.11)	5.17 (4.22–6.38)	0.973
Irregular surface, *n* (%)	22 (75.86%)	11 (17.74%)	< 0.001
Positive HIP, *n* (%)	23 (79.31%)	15 (24.19%)	< 0.001
Enhancement grade			
Grade 0, *n* (%)	0 (0%)	18 (29.03%)	< 0.001
Grade 1, *n* (%)	3 (10.34%)	27 (43.55%)	
Grade 2, *n* (%)	26 (89.66%)	17 (27.42%)	
Location			
M1, *n* (%)	26 (89.66%)	50 (80.65%)	0.251
M2, *n* (%)	3 (10.34%)	9 (14.52%)	
M3, *n* (%)	0 (0%)	3 (10.34%)	
Susceptibility (ppb)	240.00 (190.00–386.50)	-183.50 (-252.50 -56.00)	< 0.001

OWA, outer wall area; *IWA*, inner wall area; *LA*, lesion area; *LR*, lipid ratio; *HIP*, hyperintensity within plaque; *ppb*, parts per billion

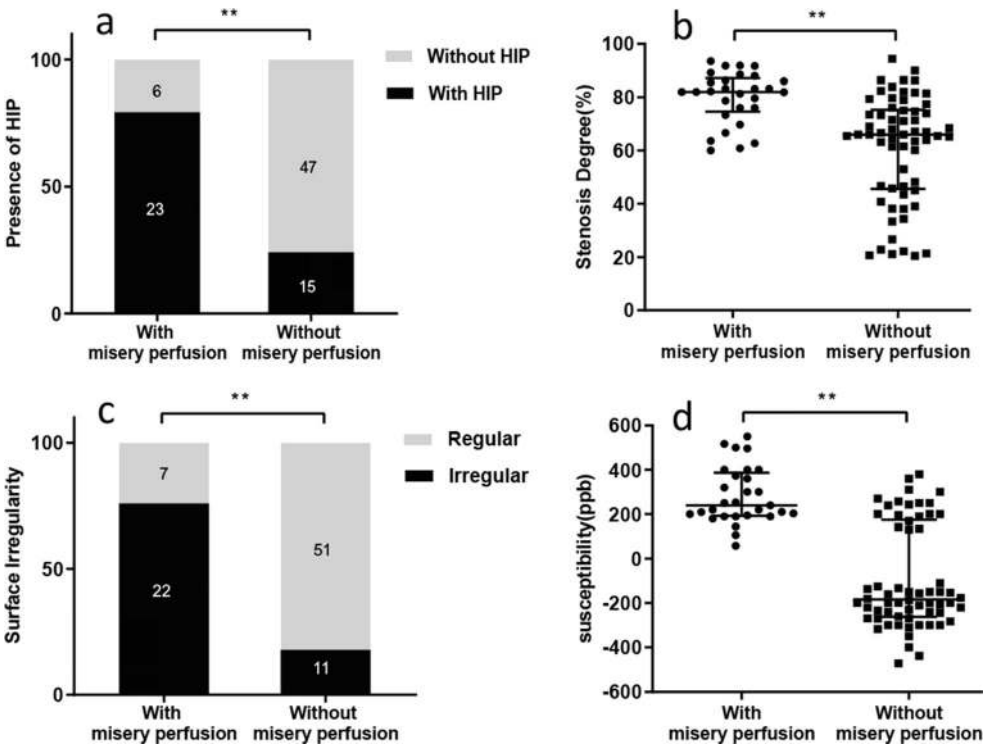

Fig. 3 Comparison between the groups with and without misery perfusion in presence of HIP (**a**), stenosis degree (**b**), surface irregularity (**c**), and susceptibility (**d**). (**$p < 0.001$)

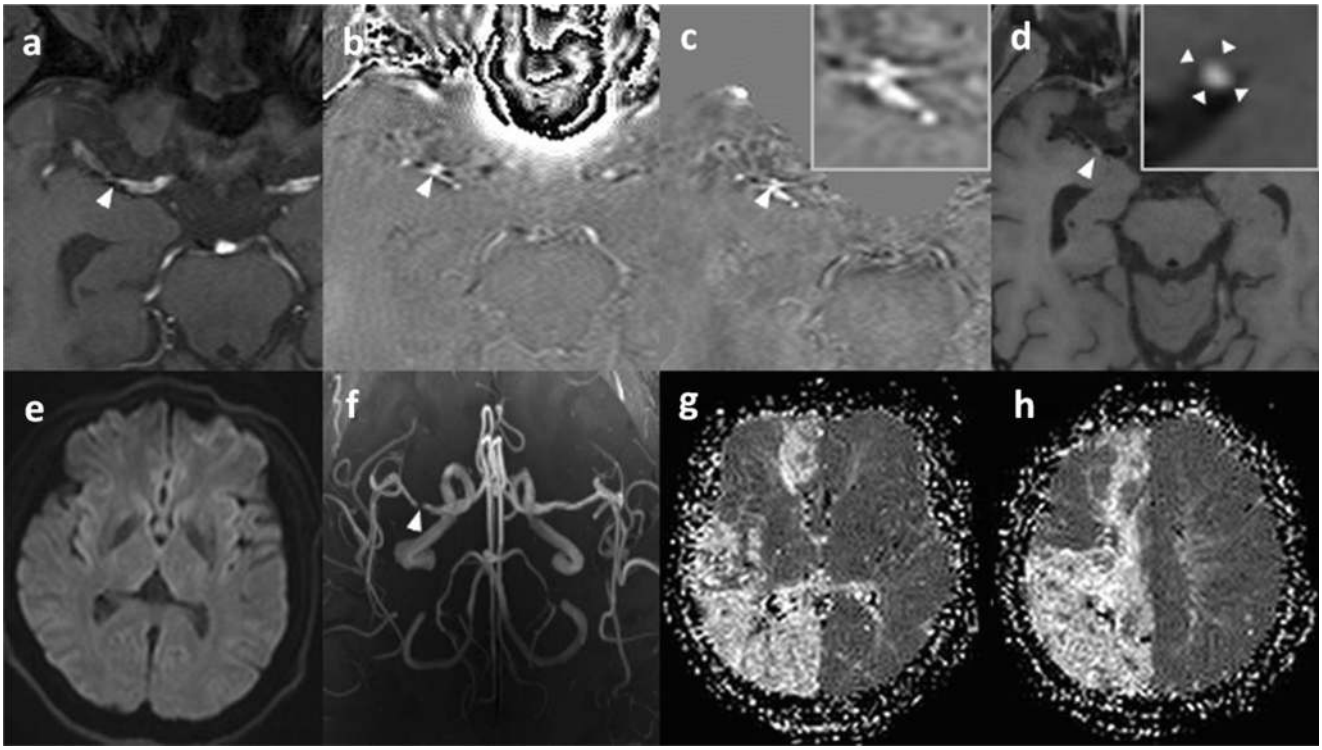

Fig. 4 A 50-year-old male with a positive susceptibility of plaque in the right M1 segment. White arrowheads indicate abnormal hypointensity on susceptibility image (**a**), and hyperintensities at the same location on HP-phase (**b**) and QSM (**c**) images; axial post-contrast vessel wall image (**d**) shows enhanced plaque in the right M1 segment (zoomed image on shows plaque with maximal luminal stenosis). DWI (**e**) shows negative finding. TOF-MRA (**f**) shows discontinuous right M1 segment (arrowhead). MTT maps (**e**, **f**) show hypoperfusion in M2, M3, M5, M6, and insular lobe. The MTT-ASPECTS of this patient is 5.

Plaque characteristics between the two groups with and without misery perfusion

As presented in Table 2 and Fig. 3, plaques in the group with misery perfusion had smaller IWA, higher stenosis degree, higher frequency of HIP and irregular surface, and higher enhancement degree ($p = 0.002$, < 0.001, < 0.001, < 0.001, < 0.001, respectively). The susceptibility values of plaques in the group with misery perfusion were significantly higher than those in the group without ($p < 0.001$), with median susceptibility of 240.00 parts per billion (ppb) (IQR, 190.00–386.50) versus -183.50 ppb (IQR, -252.50 -56.00). Case on the relationship between plaque characteristics and misery perfusion is shown in Fig. 4. No significant findings were observed in OWA, LA, lipid area, LR, and remodeling index between the two groups (Table 2).

Evaluation of plaque vulnerability using STAGE and hr-vwMRI

Ninety-one MCA plaques were identified both on hr-vwMRI and both on STAGE, as listed in Table 3. Taking hr-vwMRI as the reference, STAGE showed high consistency in detecting vulnerable plaques: based on hr-vwMRI, 46 plaques were vulnerable and 45 plaques were stable. Based on the STAGE data, 47 plaques were vulnerable, and 44 were stable. Only 5 plaques in total showed discrepancy between hr-vwMRI and STAGE in relation to plaque vulnerability. Moreover, plaque susceptibility was significantly correlated with TWV which reflects the probability of vulnerable plaques ($r_s = 0.808$, $p < 0.001$; see Supplementary Fig. 3).

Table 3 Performance of STAGE regarding detection of vulnerable plaque compared with hr-vwMRI in all plaques

	hr-vwMRI-stable ($n = 45$)	hr-vwMRI-vulnerable ($n = 46$)
STAGE-stable ($n = 44$)	42	2
STAGE-vulnerable ($n = 47$)	3	44

chi-square test: $p < 0.001$

STAGE, strategically acquired gradient echo; *hr-vwMRI*, high-resolution vessel wall MRI

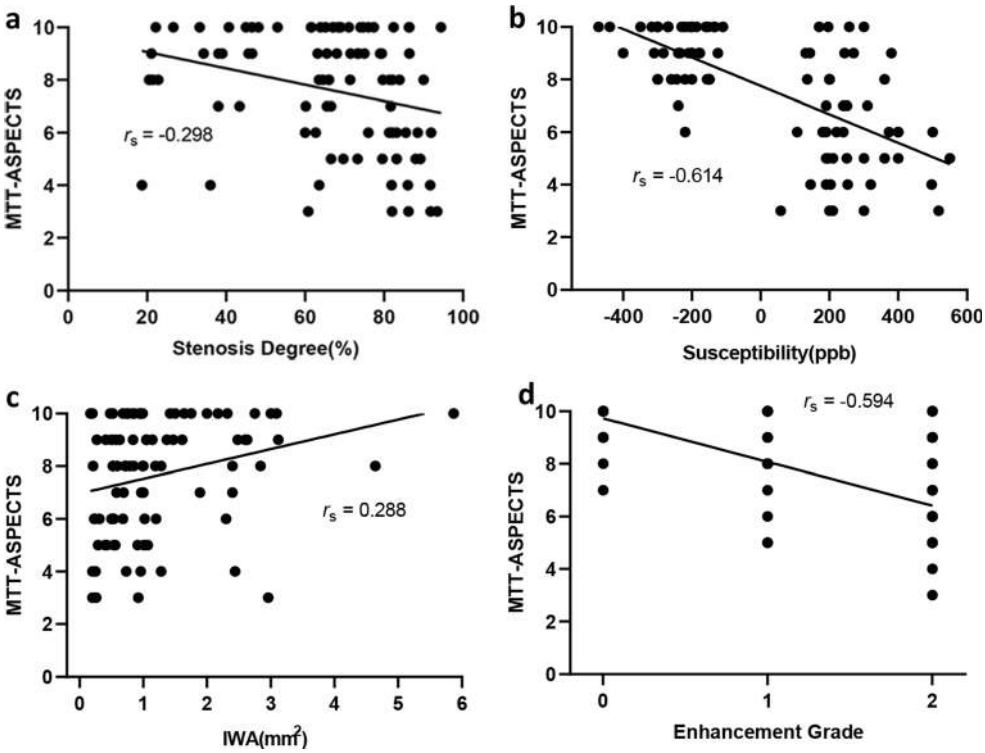

Fig. 5 The correlations between MTT-ASPECTS and stenosis degree (**a**), susceptibility (**b**), IWA (**c**), and enhancement grade (**d**)

The relationship between plaque characteristics and the presence of misery perfusion

The correlations between NIHSS, MTT-ASPECTS, and plaque characteristics were described in detail in supplementary material and Supplementary Fig. 4. As shown in Fig. 5 and Supplementary Table 4, IWA and stenosis degree were slightly correlated with MTT-ASPECTS ($r_s = 0.288, -0.298$; $p = 0.006$, 0.004), while surface irregularity, presence of HIP, enhancement grade, and susceptibility were moderately correlated with MTT-ASPECTS ($r_s = -0.580, -0.501, -0.594, -0.614$, respectively, $p < 0.001$ for all). The six variables were input for the univariate logistic analysis and entered into multivariate regression with $p < 0.05$ for all (Table 4). In the multivariate logistic analysis, only susceptibility and stenosis degree were associated with misery perfusion ($p = 0.025$, $p = 0.048$). As Fig. 6 demonstrated, for determining the presence of misery perfusion, the AUC (95% CI) for susceptibility, stenosis degree, and the combination of the two variables were 0.860 (0.771–0.924), 0.747 (0.645–0.832), and 0.900 (0.819–0.953), respectively. Detailed values are presented in Table 5.

Discussion

There were two important findings in this work. First, this study demonstrated that QSM data from STAGE-B has good efficiency in assessing MCA plaque vulnerability compared with hr-vwMRI. Second, the combination of susceptibility measured on QSM and stenosis degree

Table 4 Univariate and multivariate logistic analysis of the two groups

Variables	Univariate logistic analysis			Multivariate logistic analysis		
	OR	95% CI	*p* value	OR	95% CI	*p* value
IWA	0.403	0.196–0.831	0.014	1.006	0.360–2.813	0.990
Stenosis degree	1.054	1.020–1.089	0.002	1.052	1.000–1.105	0.048[#]
Surface irregularity	11.846	4.156–33.768	< 0.001	1.045	0.197–5.534	0.958
Presence of HIP	9.370	3.271–26.847	< 0.001	0.847	0.162–4.425	0.843
Enhancement grade	14.873	4.218–52.448	< 0.001	3.406	0.619–18.730	0.159
Susceptibility	1.008	1.004–1.011	< 0.001	1.006	1.001–1.011	0.025[#]

[#] Statistically significant; *IWA*, inner wall area; *HIP*, hyperintensity within plaque; *STAGE*, strategically acquired gradient echo; *OR*, odds ratio; *CI*, confidence interval

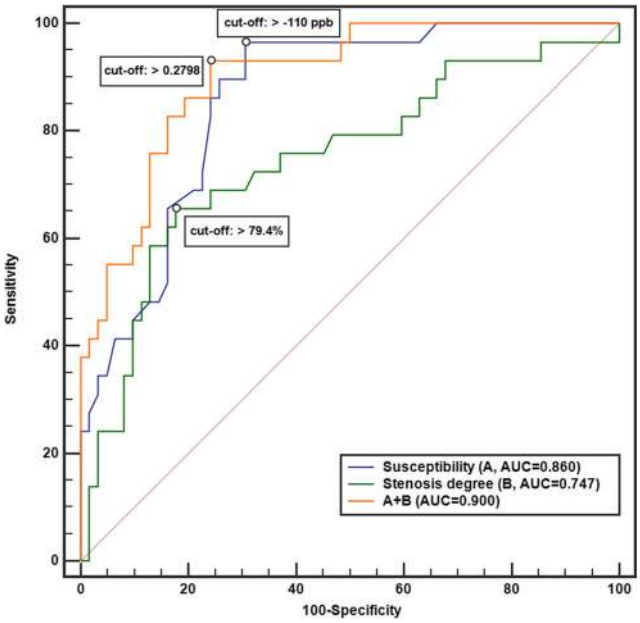

Fig. 6 ROC curve for determining the presence of misery perfusion. The AUCs for susceptibility (A), stenosis degree (B), and the combination of both (C) were 0.860, 0.747, and 0.900. The cutoff values for A, B, and C were as follows: >-110, > 79.4, > 0.2798, respectively

evaluated on hr-vwMRI has good efficiency to predict misery downstream perfusion.

Our results revealed that QSM images were sensitive to local magnetic field change caused by vulnerable intracranial plaque components. Substances with negative susceptibility in the vessel walls might be calcification and myelin, which are diamagnetic [35]. Positive susceptibility represents paramagnetic substances and in the MCA walls, it can be attributed to abundant vasa vasorum, IPH, and hemorrhage caused by plaque rupture, which are considered vulnerable plaque features [31, 36]. In our results, 44 vulnerable plaques identified both on STAGE and on hr-vwMRI with possible VV and IPH appeared bright on HP-phase and QSM images, whereas 56 stable plaques with probable calcification and lipid appeared dark. These findings are in agreement with previous studies on the walls of peripheral arteries and common carotid arteries [14, 37–39]. Furthermore, plaque susceptibility showed a positive correlation with TWV which represents the possibility of vulnerable plaque, suggesting susceptibility can also evaluate plaque vulnerability quantitatively.

Areas with prolonged MTT-ASPECTS in the perfusion maps indicate compromised but viable brain tissues due to the autoregulation mechanism, some of which may develop into infarct area in the later stage [40, 41]. Therefore, predicting misery perfusion has high value for patients' treatment. Our study indicated that susceptibility and stenosis degree might represent two possible mechanisms of hypoperfusion: artery-to-artery embolism with distal branch occlusion and severe luminal stenosis caused by in situ plaque. Severe stenosis reduces antegrade blood flow, while emboli occlusion generated by plaque rupture could affect downstream perfusion [42]. Sometimes these two mechanisms may coexist if plaque rupture results in severe in situ stenosis. Previous researches found that hyperintense plaque, irregular surface, higher stenosis grade, and grade 2 enhancement were possible markers for plaque rupture and cerebral infarction [11, 29, 32]. And in our findings, HIP, irregular surface, and higher enhancement grade had higher prevalence in the group with misery perfusion but failed to remain significant in the multivariate logistic regression. Although positive susceptibility may indicate vulnerable features, this inconsistency suggested that positive susceptibility might not share the exactly same pathological findings as strong enhancement, IPH, or irregular surface. Besides, we found plaque susceptibility was negatively correlated with MTT-ASPECTS and the ROC curve revealed that plaque with susceptibility > -110 ppb had higher likelihood of misery perfusion, suggesting the quantitative QSM analysis might provide a new biomarker in assessing the severity of cerebral ischemia.

This study has several limitations. First, this study lacked according histopathologic findings and plaque vulnerability was evaluated with hr-vwMRI as the standard. Although the results indicated that STAGE had good efficiency in detecting vulnerable plaques compared to hr-vwMRI, we could not know which technique was more efficient. In the future, multiple MR sequences and automatic analysis software for plaque components should be applied to confirm findings of STAGE and hr-vwMRI. Second, because of the field dipole effect [39], abnormal signals detected on QSM images might not reveal the actual shape of plaques. Therefore, measuring some morphological features such as plaque volume, plaque length, and stenosis degree is infeasible. Third, the number of patients included was relatively small, which might have

Table 5 Diagnostic accuracy of stenosis degree and susceptibility in differentiating occurrence of misery perfusion

	AUC	*p* value	95% CI	Cutoff	Sensitivity (%)	Specificity (%)
Susceptibility, A	0.860	< 0.001	0.771–0.924	> -110	96.55	69.35
Stenosis degree, B	0.747	< 0.001	0.645–0.832	> 79.4	65.52	82.26
A + B	0.900	< 0.001	0.819–0.953	> 0.2798*	93.10	75.81

*After adjustment

influenced efficiency of assessing plaque vulnerability for STAGE. Finally, our evaluation of cerebral perfusion impairment was restricted to MTT-ASPECTS analysis, and quantitative hypoperfusion volume was not calculated. Further studies involving the relationship between plaque quantitative susceptibility and the volume of hypoperfusion are expected to be explored.

In conclusion, we demonstrated that the QSM data from STAGE had good efficiency in evaluating the vulnerability of MCA plaques compared with hr-vwMRI. Plaques with higher susceptibility and stenosis degree were associated with the occurrence of misery perfusion, indicating the incremental value for STAGE to assess plaque characteristics in addition to hr-vwMRI.

Funding information The authors have received grant support from the National Natural Science Foundation of China, contract grant numbers: 81871342, 81901728.

Compliance with ethical standards

Guarantor The scientific guarantor of this publication is Shuang Xia.

Conflict of interest No conflict of interest declared.

Informed consent Written informed consent was waived by the Institutional Review Board.

Ethical approval Written informed consent from all subjects was obtained.

Methodology
• retrospective.
• performed at one institution.

References

1. Arenillas JF (2011) Intracranial atherosclerosis: current concepts. Stroke 42:S20–S23
2. Chen XY, Wong KS, Lam WW, Zhao HL, Ng HK (2008) Middle cerebral artery atherosclerosis: histological comparison between plaques associated with and not associated with infarct in a postmortem study. Cerebrovasc Dis 25:74–80
3. Vakil P, Vranic J, Hurley MC et al (2013) T1 gadolinium enhancement of intracranial atherosclerotic plaques associated with symptomatic ischemic presentations. AJNR Am J Neuroradiol 34:2252–2258
4. Toutouzas K, Benetos G, Karanasos A, Chatzizisis YS, Giannopoulos AA, Tousoulis D (2015) Vulnerable plaque imaging: updates on new pathobiological mechanisms. Eur Heart J 36:3147–3154
5. de Havenon A, Mossa-Basha M, Shah L et al (2017) High-resolution vessel wall MRI for the evaluation of intracranial atherosclerotic disease. Neuroradiology 59:1193–1202
6. Dieleman N, Yang W, Abrigo JM et al (2016) Magnetic resonance imaging of plaque morphology, burden, and distribution in patients with symptomatic middle cerebral artery stenosis. Stroke 47:1797–1802
7. Mossa-Basha M, Alexander M, Gaddikeri S., Yuan C, Gandhi D (2016) Vessel wall imaging for intracranial vascular disease evaluation. J Neurointerv Surg 8:1154–1159
8. Feng X, Chan KL, Lan L et al (2019) Stroke mechanisms in symptomatic intracranial atherosclerotic disease: classification and clinical implications. Stroke 50:2692–2699
9. Leng X, Lan L, Ip HL et al (2019) Hemodynamics and stroke risk in intracranial atherosclerotic disease. Ann Neurol 85:752–764
10. Ge X, Zhao H, Zhou Z et al (2019) Association of fractional flow on 3D-TOF-MRA with cerebral perfusion in patients with MCA stenosis. AJNR Am J Neuroradiol 40:1124–1131
11. Lu SS, Ge S, Su CQ et al (2018) MRI of plaque characteristics and relationship with downstream perfusion and cerebral infarction in patients with symptomatic middle cerebral artery stenosis. J Magn Reson Imaging 48(1):66–73
12. Liu S, Luo Y, Wang C et al (2020) Combination of plaque characteristics, pial collaterals, and hypertension contributes to misery perfusion in patients with symptomatic middle cerebral artery stenosis. J Magn Reson Imaging 51:195–204
13. Kerwin WS, Canton G (2009) Advanced techniques for MRI of atherosclerotic plaque. Top Magn Reson Imaging 20:217–225
14. Liu S, Buch S, Chen Y et al (2017) Susceptibility-weighted imaging: current status and future directions. NMR Biomed 30:1099-1492
15. Ciraci S, Gumus K, Doganay S et al (2017) Diagnosis of intracranial calcification and hemorrhage in pediatric patients: comparison of quantitative susceptibility mapping and phase images of susceptibility-weighted imaging. Diagn Interv Imaging 98:707–714
16. Haacke EM, Liu S, Buch S, Zheng W, Wu D, Ye Y (2015) Quantitative susceptibility mapping: current status and future directions. Magn Reson Imaging 33:1–25
17. Liu C, Li W, Tong KA, Yeom KW, Kuzminski S (2015) Susceptibility-weighted imaging and quantitative susceptibility mapping in the brain. J Magn Reson Imaging 42:23–41
18. Buch S, Chen Y, Mark Haacke E (2019) Susceptibility mapping of the dural sinuses and other superficial veins in the brain. Magn Reson Imaging 57:19–27
19. Yan F, He N, Lin H, Li R (2018) Iron deposition quantification: applications in the brain and liver. J Magn Reson Imaging 48:301–317
20. Chen Y, Liu S, Wang Y, Kang Y, Haacke EM (2018) STrategically Acquired Gradient Echo (STAGE) imaging, part I: creating enhanced T1 contrast and standardized susceptibility weighted imaging and quantitative susceptibility mapping. Magn Reson Imaging 46:130–139
21. Wang Y, Chen Y, Wu D et al (2018) STrategically Acquired Gradient Echo (STAGE) imaging, part II: correcting for RF inhomogeneities in estimating T1 and proton density. Magn Reson Imaging 46:140–150
22. Chen Y, Liu S, Buch S, Hu J, Kang Y, Haacke EM (2018) An interleaved sequence for simultaneous magnetic resonance angiography (MRA), susceptibility weighted imaging (SWI) and quantitative susceptibility mapping (QSM). Magn Reson Imaging 47:1–6
23. Schweser F, Deistung A, Lehr BW, Reichenbach JR (2011) Quantitative imaging of intrinsic magnetic tissue properties using MRI signal phase: an approach to in vivo brain iron metabolism? Neuroimage 54:2789–2807
24. Chai C, Wang H, Liu S et al (2019) Increased iron deposition of deep cerebral gray matter structures in hemodialysis patients: a longitudinal study using quantitative susceptibility mapping. J Magn Reson Imaging 49:786–799
25. Ostergaard L, Weisskoff RM, Chesler DA, Gyldensted C, Rosen BR (1996) High resolution measurement of cerebral blood flow using intravascular tracer bolus passages. Part I: mathematical approach and statistical analysis. Magn Reson Med 36:715–725

26. Padroni M, Bernardoni A, Tamborino C et al (2016) Cerebral blood volume ASPECTS is the best predictor of clinical outcome in acute ischemic stroke: a retrospective, combined semi-quantitative and quantitative assessment. PLoS One 11(1):e0147910
27. Hui FK, Obuchowski NA, John S et al (2017) ASPECTS discrepancies between CT and MR imaging: analysis and implications for triage protocols in acute ischemic stroke. J Neurointerv Surg 9:240–243
28. Samuels OB, Joseph GJ, Lynn MJ, Smith HA, Chimowitz MI (2000) A standardized method for measuring intracranial arterial stenosis. AJNR Am J Neuroradiol 21:643–646
29. Wu F, Song H, Ma Q et al (2018) Hyperintense plaque on intracranial vessel wall magnetic resonance imaging as a predictor of artery-to-artery embolic infarction. Stroke 49:905–911
30. Ye Qiao P, Steven R, Zeiler M et al (2014) Intracranial plaque enhancement in patients with cerebrovascular events on high-spatial-resolution MR images. Radiology 271:534–542
31. Yang WJ, Wong KS, Chen XY (2017) Intracranial atherosclerosis: from microscopy to high-resolution magnetic resonance imaging. J Stroke 19:249–260
32. Wu F, Ma Q, Song H et al (2018) Differential features of culprit intracranial atherosclerotic lesions: a whole-brain vessel wall imaging study in patients with acute ischemic stroke. J Am Heart Assoc 7(15):e009705
33. Lee HN, Ryu CW, Yun SJ (2018) Vessel-Wall magnetic resonance imaging of intracranial atherosclerotic plaque and ischemic stroke: a systematic review and meta-analysis. Front Neurol 9:1032
34. Kim BS, Chung PW, Park KY et al (2017) Burden of intracranial atherosclerosis is associated with long-term vascular outcome in patients with ischemic stroke. Stroke 48:2819–2826
35. Reichenbach JR, Schweser F, Serres B, Deistung A (2015) Quantitative susceptibility mapping: concepts and applications. Clin Neuroradiol 25:225–230
36. Portanova A, Hakakian N, Mikulis DJ, Virmani R, Abdalla WMA, Wasserman BA (2013) Intracranial vasa vasorum: insights and implications for imaging. Radiology 267:667–679
37. Barnes SR, Haacke EM (2009) Susceptibility-weighted imaging: clinical angiographic applications. Magn Reson Imaging Clin N Am 17:47–61
38. Raman SV, Winner MW 3rd, Tran T et al (2008) In vivo atherosclerotic plaque characterization using magnetic susceptibility distinguishes symptom-producing plaques. JACC Cardiovasc Imaging 1:49–57
39. Yang Q, Liu J, Barnes SR et al (2009) Imaging the vessel wall in major peripheral arteries using susceptibility-weighted imaging. J Magn Reson Imaging 30:357–365
40. Cianfoni A, Colosimo C, Basile M, Wintermark M, Bonomo L (2007) Brain perfusion CT: principles, technique and clinical applications. Radiol Med 112:1225–1243
41. Moskowitz MA, Lo EH, Iadecola C (2010) The science of stroke: mechanisms in search of treatments. Neuron 67:181–198
42. Bodle JD, Feldmann E, Swartz RH, Rumboldt Z, Brown T, Turan TN (2013) High-resolution magnetic resonance imaging: an emerging tool for evaluating intracranial arterial disease. Stroke 44:287–292